

Polarized Raman Spectroscopy of Double-Stranded RNA from Bacteriophage $\phi 6$: Local Raman Tensors of Base and Backbone Vibrations

James M. Benevides, Masamichi Tsuboi, Jaana K. H. Bamford, and George J. Thomas, Jr.

Division of Cell Biology and Biophysics, School of Biological Sciences, University of Missouri–Kansas City, Kansas City, Missouri 64110-2499 USA

ABSTRACT Raman tensors for localized vibrations of base (A, U, G, and C), ribose and phosphate groups of double-stranded RNA have been determined from polarized Raman measurements on oriented fibers of the genomic RNA of bacteriophage $\phi 6$. Polarized Raman intensities for which electric vectors of both the incident and scattered light are polarized either perpendicular (I_{bb}) or parallel (I_{cc}) to the RNA fiber axis have been obtained by Raman microspectroscopy using 514.5-nm excitation. Similarly, the polarized Raman components, I_{bc} and I_{cb} , for which incident and scattered vectors are mutually perpendicular, have been obtained. Spectra collected from fibers maintained at constant relative humidity in both H_2O and D_2O environments indicate the effects of hydrogen-isotopic shifts on the Raman polarizations and tensors. Novel findings are the following: 1) the intense Raman band at 813 cm^{-1} , which is assigned to phosphodiester (OPO) symmetrical stretching and represents the key marker of the A conformation of double-stranded RNA, is characterized by a moderately anisotropic Raman tensor; 2) the prominent RNA band at 1101 cm^{-1} , which is assigned to phosphodioxy (PO_2^-) symmetrical stretching, also exhibits a moderately anisotropic Raman tensor. Comparison with results obtained previously on A, B, and Z DNA suggests that tensors for localized vibrations of backbone phosphodiester and phosphodioxy groups are sensitive to helix secondary structure and local phosphate group environment; and 3) highly anisotropic Raman tensors have been found for prominent and well-resolved Raman markers of all four bases of the RNA duplex. These enable the use of polarized Raman spectroscopy for the determination of purine and pyrimidine base residue orientations in ribonucleoprotein assemblies. The present determination of Raman tensors for dsRNA is comprehensive and accurate. Unambiguous tensors have been deduced for virtually all local vibrational modes of the $300\text{--}1800\text{ cm}^{-1}$ spectral interval. The results provide a reliable basis for future evaluations of the effects of base pairing, base stacking, and sequence context on the polarized Raman spectra of nucleic acids.

GLOSSARY

D	deuterium, 2H
D_2O	deuterium oxide
dsRNA	double-stranded RNA from bacteriophage $\phi 6$
dsRNA[D]	deuterated dsRNA, in which H has been exchanged by D in D_2O solution
ssRNA	single-stranded RNA
I_{\parallel}	intensity of Raman scattering parallel to the direction of the incident electric vector
I_{\perp}	intensity of Raman scattering perpendicular to the direction of the incident electric vector
ρ	Raman depolarization ratio ($\equiv I_{\perp}/I_{\parallel}$)

INTRODUCTION

Molecular mechanisms of protein-nucleic acid recognition generally require specific hydrogen bonding or electrostatic interactions of protein side chains with accessible sites of the nucleic acid bases and nonspecific interactions with sugar or phosphate moieties of the nucleic acid backbone. Many examples of such interactions have been revealed by x-ray crystallography and multidimensional NMR spectroscopy of protein-DNA and protein-RNA complexes (Steitz, 1990). To advance our understanding of the principles governing molecular recognition in native chromosomal structures and other large supramolecular assemblies, additional biophysical probes are required. One approach suited to direct structural investigation of such assemblies is Raman spectroscopy. The Raman technique is informative of covalent bonding arrangements and of hydrogen bonding, hydrophobic, and electrostatic interactions. It is also applicable to most sample morphologies over wide ranges of experimental conditions. Applications to investigate molecular recognition in viruses (Li et al., 1990, 1993a, b) and repressor-operator complexes (Benevides et al., 1994a, b) and to elucidate mechanisms of virus assembly and disassembly (Tuma et al., 1996a–c) have been described. The Raman method has also been implemented to probe macromolecular dynamics and isotope-exchange phenomena in both protein-RNA and protein-DNA assemblies (Li et al., 1993b; Reilly and Thomas, 1994).

Received for publication 2 December 1996 and in final form 27 February 1997.

Address reprint requests to George J. Thomas, Jr., Division of Cell Biology and Biophysics, School of Biological Sciences, University of Missouri–Kansas City, Kansas City, MO 64110-2499.

This is paper LXIV in the series Raman Spectral Studies of Nucleic Acids. Supported by NIH Grant GM54378.

Dr. Tsuboi's permanent address is Department of Fundamental Science, Iwaki-Meisei University, Iwaki, Fukushima 970, Japan.

Dr. Bamford's permanent address is Biocenter, University of Helsinki, Finland.

© 1997 by the Biophysical Society

0006-3495/97/06/2748/15 \$2.00

The foremost prerequisite for implementation of Raman spectroscopy in nucleoprotein studies is reliable vibrational band assignments. If, in addition to definitive assignments, detailed information is also available on the *polarization* properties of the Raman bands, then the Raman spectrum may be further exploited to yield the directionality of specific molecular subgroups in the oriented macromolecular assembly. Recently, polarized Raman spectroscopy has been successfully employed for this purpose in studies of the filamentous DNA virus, *fd* (Overman et al., 1996; Tsuboi et al., 1996). The key to determination of residue orientation by polarized Raman spectroscopy is prior knowledge of the Raman tensors corresponding to the spectral bands of interest (for a review, see Thomas and Tsuboi, 1993).

Determination of the Raman tensors corresponding to localized vibrations of a macromolecule—such as those of base, sugar, and phosphate moieties of a nucleic acid—is experimentally challenging and computationally tedious. As a first step in this direction, the local Raman tensors for bands of guanine, cytosine, deoxyribose, and phosphate residues of *Z* DNA were determined in a polarized Raman study of the d(CGCGCG) single crystal (Benevides et al., 1993). The analysis of local DNA Raman tensors was subsequently extended to vibrations of the adenine and thymine residues and to additional modes of the deoxyribose-phosphate backbone in a polarized Raman study of oriented calf thymus DNA fibers in both *A* and *B* conformations (Thomas et al., 1995). In addition to the Raman tensors evaluated in these studies, the polarized Raman spectra of *A*, *B*, and *Z* DNA have facilitated the definitive assignment of many previously unassigned, unresolved, or poorly understood bands of the sugar-phosphate backbone. The polarized Raman results have, therefore, significantly advanced prospects for use of Raman spectroscopy as a probe of molecular structure and recognition in DNA and its complexes.

In the present work, we have determined the local Raman tensors of double-stranded (ds) RNA. This has been accomplished by a detailed analysis of polarized Raman spectra (514.5-nm laser excitation) obtained with a Raman microscope on oriented fibers of the tripartite dsRNA genome from bacteriophage $\phi 6$. Genomic $\phi 6$ dsRNA contains 55.8% GC and 44.2% AU pairs (Mindich and Bamford, 1988). Raman intensities were measured with electric vectors of both incident and scattered light polarized either perpendicular (I_{bb}) or parallel (I_{cc}) to the fiber axis. Additionally, the polarized Raman components, I_{bc} and I_{cb} , for which incident and scattered vectors are mutually perpendicular, were obtained. The polarized Raman analysis was conducted on both protonated and deuterated forms of dsRNA, the latter following deuterium-isotope (D) exchange of the fiber in a controlled deuterium oxide (D_2O) environment.

The combined polarization and deuteration analyses have facilitated the first complete Raman vibrational assignment of dsRNA, and extend the body of nucleic acid local Raman

tensors to the RNA duplex and its constituents. The results are of interest for several reasons. First, the local Raman tensors for marker bands of the ordered (*A* form) backbone of dsRNA provide, in principle, a basis for application of polarized Raman spectroscopy to elucidate RNA chain orientation in ribonucleoprotein assemblies. Second, the local Raman tensors for bands of all RNA subgroups (i.e., for vibrations of A, U, G, C, ribose, and phosphate groups) enable polarized Raman spectroscopy to be used as a probe of orientation of these groups in biological assemblies. Potential targets include transcriptional complexes, RNA viruses, viroids, hybrid RNA · DNA structures, and holoproteins that contain ribonucleotide cofactors. Third, up to the present, a detailed assignment scheme has not been established for the Raman spectrum of dsRNA of mixed-base sequence. Earlier RNA applications have focused mainly on synthetic polyribonucleotide complexes and single-stranded RNA molecules (reviewed by Thomas, 1986). Only scant data have been published on native dsRNA of well-characterized purity and base composition (Li et al., 1993b). Finally, the Raman band assignments and tensors developed here for the *A* conformation of $\phi 6$ dsRNA augment and improve upon those reported previously for the *A* conformation of DNA (Thomas et al., 1995). Comparison of the results obtained on *A* RNA and *A* DNA indicates a number of contrasting differences in Raman polarizations and tensors and suggests an interesting spectroscopic basis for differentiating the two double-helical structures. A significant advantage of *A* RNA over *A* DNA as a target for quantitative spectroscopic analysis is its relative resistance to polymorphism. Obtaining fiber specimens of *A* DNA that are uncontaminated by *B* DNA or other conformations is known to be highly problematic (Brandes et al., 1989; Thomas et al., 1995).

METHODS

Local Raman tensors of dsRNA

In the off-resonance Raman effect, the intensity of each spectral band is determined by the change of polarizability associated with the corresponding molecular normal mode of vibration. This Raman intensity can be expressed in terms of the principal elements, α_{xx} , α_{yy} , and α_{zz} , of the derived polarizability tensor (Raman tensor), where the derivatives are taken with respect to the vibrational normal coordinate, and *x*, *y*, and *z* are the tensor principal axes. In the absence of molecular symmetry, the principal axes will be oriented differently and the relative magnitudes of α_{xx} , α_{yy} , and α_{zz} will also generally differ for each normal mode of vibration (i.e., for each experimentally observed spectral band). It should be kept in mind that each Raman band assigned to a particular vibrational mode actually represents a superposition of contributions from all identical subgroups in the macromolecule. Thus, a band assigned to a particular normal mode of the phosphate group, such as the 1100 cm^{-1} band assigned to the PO_2^- symmetrical stretching mode, is representative of all phosphates in the RNA duplex; similarly, a band assigned to a uracil vibration arises from all uracils in the RNA, etc. Further discussion of nucleic acid Raman tensors has been given by Benevides et al. (1993) and Thomas et al. (1995).

Here, the specific objectives are to determine the orientations of the Raman tensor principal axes (*x*, *y*, *z*) and the relative magnitudes ($r_1 \equiv \alpha_{xx}/\alpha_{zz}$ and $r_2 \equiv \alpha_{yy}/\alpha_{zz}$) of the tensor components corresponding to the

most prominent of the ~40 or so Raman bands observed in spectra of normal and deuterated dsRNA.

For each nucleotide unit of the oriented dsRNA fiber, we employ a rectangular coordinate system (**X**, **Y**, **Z**) with **Z** parallel to the fiber axis (**c**) and **X** and **Y** perpendicular to **c**. The Raman tensor for a vibrational mode localized in the nucleotide unit is characterized by the three components, α_{xx} , α_{yy} , α_{zz} , defined above. The Raman tensor components in the **XYZ** coordinate system (α_{xx} , α_{yy} , α_{zz}) are related by direction cosines to those of the **xyz** system, as shown previously (Thomas et al., 1995). Because the **X**, **Y**, and **Z** coordinates of each nucleotide unit are located along a helical axis, it is convenient to introduce the complex coordinates: $a_+ = (X + iY)/\sqrt{2}$, $a_- = (X - iY)/\sqrt{2}$ and $a_0 = Z$. In terms of these coordinates, the Raman tensor components form a Hermitian matrix with elements a_0 ($\equiv [\alpha_{xx} + \alpha_{yy}]/2$), a_1 ($\equiv \alpha_{zz}$), a_2 ($\equiv [\alpha_{zx} + i\alpha_{yz}]/\sqrt{2}$), and a_3 ($\equiv [\alpha_{xx} - \alpha_{yy} + 2i\alpha_{xy}]/2$) (Thomas et al., 1995). As shown by Higgs (1953), the Raman selection rules and polarization intensities for the helical residues are governed by the relations listed in Table 1.

Raman depolarization ratio

The Raman depolarization ratio (ρ), which is defined for a Raman band of randomly oriented molecules, as in the case of an aqueous solution, is the ratio of Raman scattering intensities in directions perpendicular (I_{\perp}) and parallel (I_{\parallel}) to the direction of polarization of the exciting radiation. A detailed examination of Raman depolarization ratios for H₂O and D₂O solutions of ribonucleotides of A, C, G, and U has been reported recently (Ueda et al., 1993). Each depolarization ratio is related to r_1 and r_2 by Eq. 1 (Tsuboi et al., 1991):

$$\rho = I_{\perp}/I_{\parallel} = \frac{1.5\{(r_1 - r_2)^2 + (r_2 - 1)^2 + (1 - r_1)^2\}}{5(r_1 + r_2 + 1)^2 + 2\{(r_1 - r_2)^2 + (r_2 - 1)^2 + (1 - r_1)^2\}} \quad (1)$$

The relationship of ρ to r_1 and r_2 can be visualized using a contour map (Thomas and Tsuboi, 1993). Such maps are helpful for determining values of r_1 and r_2 consistent with the observed values of ρ , and have been used to locate the principal axes of local Raman tensors of nucleic acids (Tsuboi et al., 1991; Benevides et al., 1993; Thomas et al., 1995).

EXPERIMENTAL PROCEDURES

Isolation and purification of $\phi 6$ dsRNA

The $\phi 6$ virus was grown, concentrated, and purified as described previously (Olkkonen et al., 1991). The RNA purification procedure includes the removal of the viral spike protein by treatment with butylated hydroxytoluene, solubilization of the viral membrane by treatment with Triton X-114, and separation of the aqueous phase containing the viral nucleocapsid. For RNA extraction, the nucleocapsid concentration in the aqueous phase (20 mM Tris-HCl, pH 7.4, 100 mM NaCl) was adjusted to 0.6 mg

protein/ml. The nucleocapsid preparation was extracted three times with phenol saturated with 100 mM Tris-HCl, pH 6.0. The residual phenol was removed by extracting the aqueous phase five times with ether. The aqueous dsRNA was precipitated by the addition of sodium chloride (to 300 mM) and three volumes of cold (-20°C) ethanol. The precipitate was collected immediately by microcentrifugation (14,000 rpm, 15 min, 4°C). The resulting pellet was washed with 75% (v/v) ethanol and dried under vacuum. The concentration, purity, and integrity of the dsRNA were analyzed by optical density measurement ($A_{260/280}$) and agarose gel electrophoresis. Approximately 5 mg of dsRNA was obtained from 8 l virus culture.

Preparation of samples for Raman spectroscopy

The double-stranded RNA was dissolved to a final concentration of 15 $\mu\text{g}/\mu\text{l}$ in deionized water and the pH was adjusted to 7.0 ± 0.1 with 0.1 M NaOH. Fibers were drawn from a drop of the solution using a standard fiber pulling device. Fibers were mounted in a tightly sealed microsample cell in which temperature and relative humidity (RH) were maintained at 10°C and 75%, respectively. Details of the microsampling apparatus have been described previously (Benevides et al., 1993). Fibers were preequilibrated for several days at room temperature and 75% RH before spectra were acquired. The polarized spectra of fibers were supplemented by depolarization ratio measurements on solutions of dsRNA dissolved to 30 $\mu\text{g}/\mu\text{l}$ in 100 mM NaCl at pH 7.

Deuterium exchange of dsRNA fibers was accomplished by replacing the saturated NaClO₃/H₂O solution in the microsample chamber with the corresponding D₂O solution. The progress of H \rightarrow D exchange was followed by monitoring the shift of the adenine ring mode near 725 cm^{-1} (H₂O) to 715 cm^{-1} (D₂O). Complete deuteration, confirmed by the symmetry of the 715 cm^{-1} band and by the absence of Raman bands of H₂O or HOD, was achieved usually within 48 h of exposure of the fiber to the D₂O atmosphere. The dsRNA deuterated in this manner is referred to hereafter as dsRNA(D).

Raman instrumentation

Raman spectra of dsRNA fibers were collected on a Raman microscope (Olympus, Model BHSM, Lake Success, NY) that was optically coupled to a triple spectrograph (ISA/Jobin Yvon Model S3000, Edison, NJ) fitted with a liquid nitrogen-cooled ISA Spectraview-2D charge-coupled-device (CCD) detector. An 80X Olympus ULWD MS Plan objective served to both focus the incident laser beam on the sample and collect the Raman scattering. Before laser excitation, the fiber was examined with a 10X objective (Olympus Neo S Plan) and cross-polarizers to determine the best location along the length of the fiber for data sampling. The 514.5 nm line from a Coherent Innova argon laser (Santa Clara, CA) served as the excitation source. The radiant power of the laser was maintained below 15 mW at the sample. Spectra of dsRNA solutions were obtained on a scanning double-monochromator (Spex Ramalog V/VI, Edison NJ). Further details of the instrumentation and sample handling for fiber and solution Raman spectroscopy have been described (Li et al., 1981; Thomas et al., 1995).

Data collection and processing

Detailed descriptions of data collection protocols for fibers and solutions of nucleic acids have been given elsewhere (Benevides et al., 1993; Thomas et al., 1995). Briefly, the electric vector of the incident radiation was directed along the laboratory X' axis as defined in Fig. 1. A polarizer, located in front of the entrance slit of the spectrograph, was used to select for Raman scattering along either the X' or Y' axis. Different Raman polarizations were obtained by rotating the fiber rather than the electric vector of the incident beam. This minimizes optical polarization artifacts and simplifies the data processing. The long axis (c axis) of the fiber was placed along either the laboratory X' or Y' axis (Fig. 1). Raman intensities

TABLE 1 Raman selection rules and intensities for a helical molecule

Polarization		Symmetry	Phase angle*	Intensity
Incident	Scattered			
c	c	A	0	$(a_0)^2$
b	b	A	0	$(a_0)^2$
a	b	E ₂	2 ψ	$1/2 a_2 ^2$
c	b	E ₁	ψ	$ a_1 ^2$
b	c	E ₁	ψ	$ a_1 ^2$

*For dsRNA, $\psi \approx 33^{\circ}$ (Arnott et al., 1972).

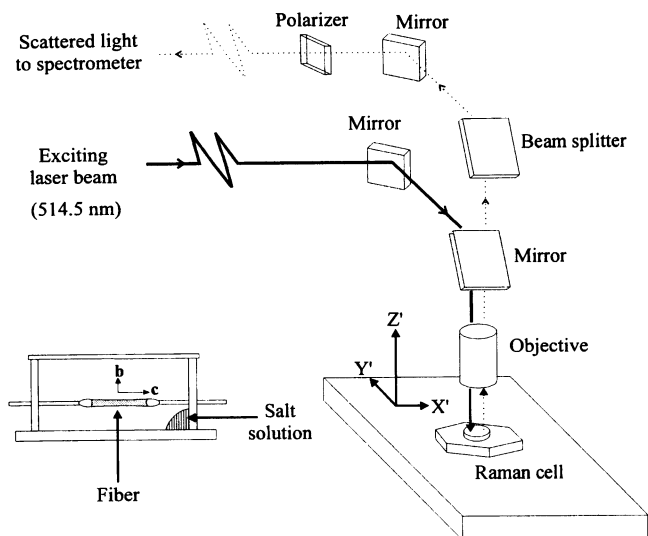


FIGURE 1 Diagram of the Raman microscope employed for collection of Raman scattering at 180° (backscattering) from an oriented fiber of RNA. The fiber is maintained at constant relative humidity by a saturated salt solution in a thermostated hygrostatic cell (lower left). The laboratory coordinate system (X' , Y' , Z') provides the frame of reference for the fiber axis (c) and for the directions of polarization of electric vectors of incident and scattered light (bb , cc , bc and cb), as described in the text.

were measured in the cc (I_{cc}), bb (I_{bb}), bc (I_{bc}), and cb (I_{cb}) orientations. Spectra corresponding to different polarizations were compared only if obtained from the same fiber. The spectra displayed below represent averages of 20 exposures, each obtained with an integration time of 120 s per exposure at a spectral resolution of $\approx 6 \text{ cm}^{-1}$.

RESULTS AND DISCUSSION

Polarized Raman spectra of dsRNA and deuterated dsRNA

Polarized Raman spectra obtained from an oriented fiber of dsRNA are shown in Fig. 2. The polarized Raman intensity ratios, I_{bb}/I_{cc} and I_{bb}/I_{bc} , measured directly from these spectra are listed in Table 2. Corresponding polarized Raman spectra and intensity ratios obtained from the deuterated dsRNA fiber, following complete protium \rightarrow deuterium exchange in an atmosphere of D_2O , are given in Fig. 3 and Table 3. (Deuterated dsRNA is hereafter referred to by the notation dsRNA[D].)

Overview of the I_{bb} and I_{cc} polarized Raman spectra

Vibrations in the region $200\text{--}600 \text{ cm}^{-1}$

Bands below 600 cm^{-1} in Raman spectra of nucleic acids and other biomolecules typically have not been well characterized. This reflects in part the technical difficulties associated with collection of Raman scattered light, which is close in frequency to the laser excitation frequency, and in part the presumption that vibrational modes below 600 cm^{-1} are not particularly useful for structural diagnostics.

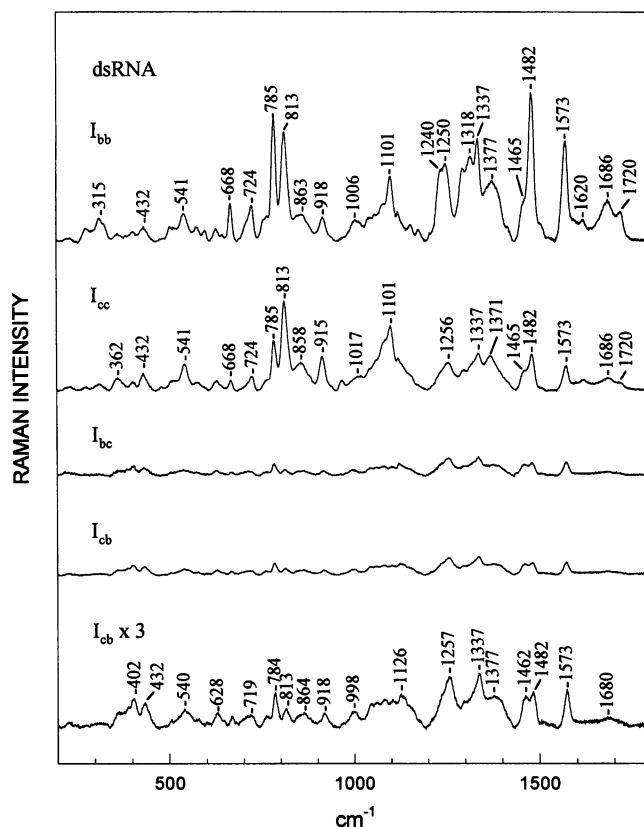


FIGURE 2 Raman spectra (I_{bb} , I_{cc} , I_{bc} , and I_{cb} , from top to bottom) obtained from a fiber of $\phi 6$ dsRNA employing polarizations bb , cc , bc and cb , respectively. In the bottom trace, the ordinate of the I_{cb} spectrum is expanded threefold. Spectra were obtained with 514.5 nm excitation on a Jobin-Yvon S3000 spectrometer equipped with an Olympus BH2 microscope (Fig. 1). Other experimental details are given in the text.

An exception is the region below 200 cm^{-1} , which contains delocalized helix modes and lattice vibrations. Both experimental and theoretical studies of the very low frequency region have been reported for Raman spectra of DNA and related polynucleotides (Lamba et al., 1989; Urabe et al., 1985).

The Raman spectrum of dsRNA (Fig. 2) contains bands at 232, 278, 315, 362, 404, 432, 503, 541, 576, and 598 cm^{-1} . Of these, only the bands at 278, 315, and 598 cm^{-1} exhibit large polarized Raman intensity ratios, i.e., $I_{bb}/I_{cc} \gg 1$; the remaining seven bands of the $200\text{--}600 \text{ cm}^{-1}$ interval have values within the range $0.5 < I_{bb}/I_{cc} < 2.0$ (Table 2).

For the fiber of dsRNA[D], the bands of the $200\text{--}600 \text{ cm}^{-1}$ interval are largely conserved in their frequencies and I_{bb}/I_{cc} values (Fig. 3 and Table 3). Thus, all of the bands, with the possible exception of the 598 cm^{-1} band, may be confidently assigned to similar vibrations in both protonated and deuterated RNA, which do not involve appreciable motions of exchangeable hydrogen atoms. Comparison with polarized and unpolarized Raman spectra of A DNA and B DNA fibers (Prescott et al., 1984; Thomas et al., 1995) and with data on phosphodiester model compounds (Guan and Thomas, 1996a, b) leads to the more specific assignments indicated in Tables 2 and 3.

TABLE 2 Polarized Raman intensity ratios of dsRNA fibers and depolarization ratios (ρ) of isotropic dsRNA in H₂O solution

Band (cm ⁻¹)	Assignment	I_{bb}/I_{cc}	I_{bb}/I_{bc}	ρ
232	—	1.02 ± 0.14	0.23 ± 0.03	
278	—	3.66 ± 0.51	18.9 ± 2.10	
315	A	3.58 ± 0.25	16.0 ± 1.80	
362	O—P—O + PO ₂ ⁻ bend	0.57 ± 0.08	14.2 ± 1.60	0.75 ± 0.18
404	C5'—O—P bend	1.03 ± 0.14	0.93 ± 0.13	0.47 ± 0.11
432	C3'—O—P bend	0.84 ± 0.12	1.62 ± 0.18	0.27 ± 0.05
503s	PO ₂ ⁻ scissor	1.45 ± 0.20	6.05 ± 0.85	0.18 ± 0.04
541	backbone	1.02 ± 0.07	4.71 ± 0.33	0.21 ± 0.04
576	C=O bend (C, G)	1.77 ± 0.25	5.82 ± 0.81	0.48 ± 0.14
598	C, G	2.77 ± 0.39	6.04 ± 0.85	
629	C	1.26 ± 0.18	2.62 ± 0.37	0.31 ± 0.09
645	C, A	1.27 ± 0.18	2.74 ± 0.38	
668	ring breathing (G)	3.69 ± 0.41	11.8 ± 1.30	0.08 ± 0.02
715s	ribose	2.66 ± 0.37	5.98 ± 0.84	0.30 ± 0.07
724	ring breathing (A)	2.55 ± 0.28	10.1 ± 1.10	0.09 ± 0.02
759s	C	3.78 ± 0.53	6.44 ± 0.90	
766	—	2.26 ± 0.32		0.22 ± 0.04
785	ring breathing (C, U)	2.47 ± 0.10	10.8 ± 0.65	0.12 ± 0.02
813	O—P—O stretch	1.23 ± 0.05	18.0 ± 0.72	0.05 ± 0.01
848	ribose or O—P—O stretch	1.02 ± 0.07	6.98 ± 0.77	0.13 ± 0.03
863	furanose C—O, C—C stretch	0.98 ± 0.07	5.93 ± 0.65	
874s	furanose C—O, C—C stretch	1.27 ± 0.18	7.07 ± 0.99	0.17 ± 0.05
918	furanose C—O, C—C stretch	0.69 ± 0.05	5.29 ± 0.58	0.15 ± 0.03
1045	furanose C—O, C—C stretch	1.11 ± 0.08	3.22 ± 0.37	
1058	C—O stretch	0.88 ± 0.06	3.29 ± 0.36	
1082s	—	0.75 ± 0.05	4.21 ± 0.46	0.23 ± 0.06
1101	PO ₂ ⁻ symmetric stretch	1.00 ± 0.04	8.02 ± 0.80	0.15 ± 0.04
1157	C	0.94 ± 0.07		0.48 ± 0.12
1240s	ring mode (U)	3.68 ± 0.22		0.44 ± 0.08
1250	ring mode (C, U, A)	2.80 ± 0.17	4.74 ± 0.28	0.44 ± 0.08
1297	ring mode (C, A)	3.58 ± 0.36	8.69 ± 0.87	0.36 ± 0.09
1318	ring mode (G)	2.93 ± 0.18	7.48 ± 0.75	0.38 ± 0.11
1337	ring mode (A)	2.71 ± 0.16	5.72 ± 0.34	0.42 ± 0.07
1377	ring mode (A, G, C)	1.71 ± 0.10	5.75 ± 0.58	0.40 ± 0.06
1418	ring mode (A, G, C)	1.58 ± 0.22	6.19 ± 0.87	0.65 ± 0.16
1465s	C5'H ₂ scissor	2.12 ± 0.23	4.32 ± 0.48	0.59 ± 0.14
1482	ring mode (G, A)	4.03 ± 0.24	13.1 ± 0.78	0.16 ± 0.02
1573	ring mode (A, G)	4.03 ± 0.24	7.98 ± 0.48	0.37 ± 0.05
1686	C=O stretch (U)	3.21 ± 0.35	13.3 ± 1.50	
1720	C=O stretch (G)	3.88 ± 0.43	18.6 ± 2.10	

Experimental intensity ratios, I_{bb}/I_{cc} and I_{bb}/I_{bc} , are from spectra of Fig. 2. Abbreviation: s, shoulder.

Base vibrations in the region 600–800 cm⁻¹

Base vibrations in the region 600–800 cm⁻¹ have been assigned to ring-breathing motions (Lord and Thomas, 1967; Thomas, 1970). In RNA, diagnostic bands are expected for guanine at 668 cm⁻¹, for adenine at 724 cm⁻¹, and for both cytosine and uracil at 785 cm⁻¹. These markers occur prominently in spectra of $\phi 6$ dsRNA (Fig. 2 and Table 2) and exhibit the expected deuteration shifts (Fig. 3 and Table 3). As also observed for A and B DNA (Thomas et al., 1995), each ring-breathing mode of dsRNA is characterized by $I_{bb} > I_{cc}$, consistent with the out-of-plane tensor component (α_{zz}) being significantly smaller than the in-plane components (α_{xx} , α_{yy}). However, many significant differences occur between dsRNA and dsDNA in the magnitudes of these intensity quotients. Detailed discussions are given in subsequent sections.

Interestingly, the value of I_{bb}/I_{cc} for the 668 cm⁻¹ marker of dsRNA is ~20% smaller than that of the corresponding

band (664 cm⁻¹) of dsRNA[D]. Conversely, values of I_{bb}/I_{cc} for ring-breathing modes of A and C/U are barely affected by deuteration. Guanine is also exceptional in that the deuteration shift in ring frequency is rather small (-4 cm⁻¹) in comparison to those of A and C/U (-8 cm⁻¹). A plausible explanation, supported by normal coordinate calculations (Tsuboi et al., 1973), is that only in the case of guanine does the normal mode involve appreciable motion of the glycosidic nitrogen (N9), which provides the opportunity for significant vibrational coupling with the attached furanose ring.

Backbone vibrations in the region 750–1100 cm⁻¹

Detailed assignments and discussion of backbone vibrations in this spectral region have been given previously for dsDNA (Thomas et al., 1995). In the case of dsRNA, the principal Raman marker of phosphodiester conformation is

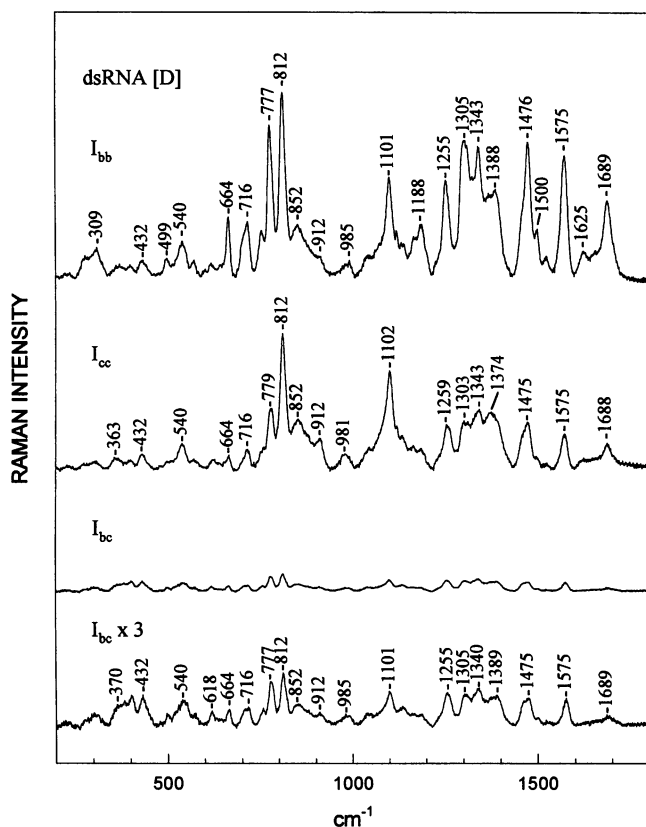


FIGURE 3 Raman spectra (I_{bb} , I_{cc} , and I_{bc} , from top to bottom) obtained from a deuterated fiber of $\phi 6$ dsRNA employing polarizations bb , cc , and bc , respectively. In the bottom trace, the ordinate of the I_{bc} spectrum is expanded threefold. Other conditions are as given in Fig. 2.

the band at 813 cm^{-1} , for which $I_{bb}/I_{cc} = 1.23$. The corresponding band of A DNA occurs at 807 cm^{-1} and has $I_{bb}/I_{cc} = 1.57$. The differences in Raman frequency and polarization between RNA and DNA are small but significant. In combination with the complementary I_{bb}/I_{bc} data (Table 2), the first tensor determination for this A backbone marker has been accomplished (see Properties of Raman tensors).

Bands at 848, 863, 874, 918, 1045, 1058, 1082, and 1101 cm^{-1} are also assigned to vibrations localized in the sugar-phosphate backbone. A similar band pattern is observed for A DNA (Thomas et al., 1995). Only the band near 900 cm^{-1} (918 cm^{-1} in RNA and 882 cm^{-1} in DNA) exhibits a Raman polarization ratio $I_{bb}/I_{cc} < 1$, presumably reflecting a similar type of vibration of the C3'-endo sugar ring in both A RNA and A DNA.

Base vibrations in the region $1100\text{--}1700\text{ cm}^{-1}$

Bands in this region of the Raman spectrum arise primarily from conjugated single- and double-bond stretching vibrations of the base residues, including exocyclic C=O and C—NH₂ groups. The spectral profile of dsRNA is markedly different from that of dsDNA (Thomas et al., 1995), owing to the replacement of thymine by uracil and sugar-specific vibrational coupling with the bases. In the I_{bb} spectrum of

Fig. 2, eight intense peaks are clearly resolved at 1240 (U), 1250 (C, U, A), 1297 (C, A), 1318 (G), 1337 (A), 1377 (A, G, C), 1482 (G, A), and 1573 cm^{-1} (A, G). Many of these bands are sensitive to deuterium exchange of exocyclic imino and amino protons (Lord and Thomas, 1967), as evidenced by the different pattern of peaks in dsRNA[D] at 1188 (A, G, C), 1255 (C, U, A), 1305 (C, A), 1343 (A), 1388 (A, G, C), 1476 (G, A), 1500 (C), and 1575 cm^{-1} (A, G) (Fig. 3). The I_{cc} spectra of Figs. 2 and 3 show that all of these bands are characterized by relatively large polarized Raman intensity ratios ($I_{bb}/I_{cc} \gg 1$), indicating small α_{zz} tensor components.

Comparison of the I_{bb}/I_{cc} values for these ring vibrations of dsRNA with those of corresponding bands of A and B DNA (Thomas et al., 1995) indicates a number of differences. In some cases the polarized Raman intensity ratios of dsRNA are intermediate between those of A and B DNA (e.g., 1482 and 1573 cm^{-1} bands); in others they are less than those of both A and B DNA (e.g., 1250 and 1337 cm^{-1} bands). The lower polarizations of dsRNA may reflect differences in base tilt and/or roll angles of RNA and DNA duplexes.

Overview of the I_{bc} and I_{cb} polarized Raman spectra

The I_{bc} (and I_{cb}) polarized Raman scattering from an oriented fiber or crystal, though expectedly feeble in intensity, is an essential complement to I_{bb} and I_{cc} spectra for determining the Raman tensor ratios r_1 and r_2 . This has been demonstrated for the case of the Z-DNA crystal, d(CGCGCG) (Benevides et al., 1993). In the absence of an acceptable I_{bc} or I_{cb} spectrum, one must rely instead on solution depolarization ratios to complement the I_{bb} and I_{cc} spectra, whence tensor parameters consistent with the solution depolarization data may be inferred. This was the case in our previous study of oriented DNA fibers (Thomas et al., 1995), which did not yield acceptable I_{bc} or I_{cb} data. However, because the A DNA backbone is not stable in solution, depolarization ratios for bands due to vibrations of the A-form backbone cannot be obtained. Accordingly, reliance upon solution depolarization ratios severely limited the number of Raman bands of A DNA that could be characterized tensorially in the previous work.

In the present study, on the other hand, I_{bc} spectra of very high signal-to-noise quality have been collected from oriented fibers of dsRNA (Fig. 2) and its deuterated counterpart, dsRNA[D] (Fig. 3). These data have provided the first opportunity to reliably determine the Raman tensors for local vibrations of the A-form sugar-phosphate backbone.

The I_{bc} intensities for all prominent Raman bands of dsRNA and dsRNA[D] are presented in Tables 2 and 3, respectively, in the form of the quotient I_{bb}/I_{bc} . These results, when combined with the I_{bb}/I_{cc} data, provide a basis for more accurate tensor determinations than previously possible (Thomas et al., 1995). Only Raman bands with

TABLE 3 Polarized Raman intensity ratios of deuterated dsRNA fibers and depolarization ratios (ρ) of isotropic dsRNA in D₂O solution

Band (cm ⁻¹)	Assignment	I_{bb}/I_{cc}	I_{bb}/I_{bc}	ρ
232	—			
279	—	4.45 ± 0.49	12.3 ± 1.35	
309	—	4.15 ± 0.25	8.56 ± 0.94	
370	O—P—O + PO ₂ ⁻ bend	1.06 ± 0.15	1.63 ± 0.18	
399	C5'—O—P bend	1.42 ± 0.20	1.21 ± 0.13	0.54 ± 0.13
432	C3'—O—P bend	1.00 ± 0.14	1.51 ± 0.17	0.18 ± 0.03
499	PO ₂ ⁻ scissor	2.25 ± 0.32	4.50 ± 0.63	
540	backbone	1.30 ± 0.09	4.24 ± 0.30	0.07 ± 0.02
571	C=O bend (C, G)	1.57 ± 0.22	4.93 ± 0.69	0.35 ± 0.10
616	C	1.20 ± 0.17	2.65 ± 0.37	0.50 ± 0.14
664	ring breathing (G)	4.60 ± 0.51	11.2 ± 1.23	0.07 ± 0.02
706	ribose	3.74 ± 0.41	8.61 ± 0.95	0.40 ± 0.11
716	ring breathing (A)	2.74 ± 0.19	9.43 ± 1.04	0.23 ± 0.05
754	C	2.03 ± 0.22	9.86 ± 1.08	0.31 ± 0.09
777	ring breathing (C, U)	2.50 ± 0.15	10.3 ± 0.62	0.14 ± 0.02
812	O—P—O stretch	1.23 ± 0.05	18.0 ± 0.72	0.05 ± 0.01
852	ribose or O—P—O stretch	0.99 ± 0.07	8.27 ± 0.91	0.13 ± 0.03
912	furanose C—O, C—C stretch	0.57 ± 0.06	5.53 ± 0.77	0.14 ± 0.03
985	furanose C—O, C—C stretch	1.01 ± 0.14	6.08 ± 0.85	0.71 ± 0.17
1043	furanose C—O, C—C stretch	1.27 ± 0.18	7.56 ± 0.83	0.43 ± 0.10
1101	PO ₂ ⁻ symmetric stretch	1.03 ± 0.04	9.04 ± 0.54	0.22 ± 0.06
1137	U	1.01 ± 0.07	5.43 ± 0.76	0.52 ± 0.11
1170	A, U, G, C	1.71 ± 0.19	9.89 ± 1.09	
1188	A, G, C (ND ₂ scissor)	2.57 ± 0.28	14.9 ± 1.64	
1255	ring mode (C, U, A)	2.26 ± 0.14	8.67 ± 0.52	
1305	ring mode (C, A)	2.94 ± 0.18	13.8 ± 0.82	
1343	ring mode (A)	2.20 ± 0.13	11.0 ± 0.66	0.64 ± 0.10
1372	ring mode (A, G)	1.43 ± 0.10	9.12 ± 0.64	
1388	ring mode (A, G, C)	1.70 ± 0.10	9.00 ± 0.54	0.65 ± 0.10
1462	C5'H ₂ scissor	2.91 ± 0.32	15.7 ± 1.73	0.27 ± 0.05
1476	ring mode (G, A)	4.03 ± 0.24	13.1 ± 0.78	0.16 ± 0.03
1500	ring mode (C)	3.75 ± 0.41	19.5 ± 2.15	
1526	ring mode (A, C)	3.42 ± 0.48	22.3 ± 3.12	
1575	ring mode (A, G)	3.43 ± 0.21	15.5 ± 0.93	0.39 ± 0.06
1625	A, U	3.55 ± 0.39	53.3 ± 7.46	0.28 ± 0.05
1689	C=O stretch (U, G)	3.13 ± 0.34	26.6 ± 2.66	0.25 ± 0.05

Experimental intensity ratios, I_{bb}/I_{cc} and I_{bb}/I_{bc} , are from spectra of Fig. 3.

anisotropic tensors can be exploited in polarized Raman spectroscopy to determine subgroup orientations in biological assemblies (Tsuboi et al., 1996). Overall, the present results indicate that a large number of Raman bands of dsRNA in particular, and of A-form nucleic acids in general, should be of value in assessing backbone orientation. This includes bands of the region 200–600 cm⁻¹, which are also demonstrated here as diagnostic of nucleic acid secondary structure.

Properties of Raman tensors for specific local vibrations of dsRNA

In order to locate the Raman tensors r_1 and r_2 for a particular Raman band, the coordinate system (i.e., set of principal axes) for the tensor components must be defined. We have employed three different coordinate systems for the purine ring (G1, G2, and G3), three for the pyrimidine ring (C1, C2, and C3) and one each for the orthophosphate group

(P1) and ribose (R1) ring. Principal axes for these coordinate systems are defined in Table 4 and illustrated in Fig. 4.

The effective shapes of the local Raman tensors associated with Raman bands of dsRNA and dsRNA[D] are presented in Tables 5 and 6, respectively. For each band in

TABLE 4 Principal axes for localized vibrational modes of dsRNA

RNA residue	Coordinate system*	Reference atoms		
		A	E1	E2
Purine	G1	N3	N1	N9
	G2	N3	N1	N7
	G3	N3	C2	N7
Pyrimidine	C1	N1	N3	C5
	C2	N1	C2	C5
	C3	N1	C2	C4
Phosphate	P1	P	O ⁻	O ⁻
Ribose	R1	O4'	C2'	C3'

*See Fig. 5.

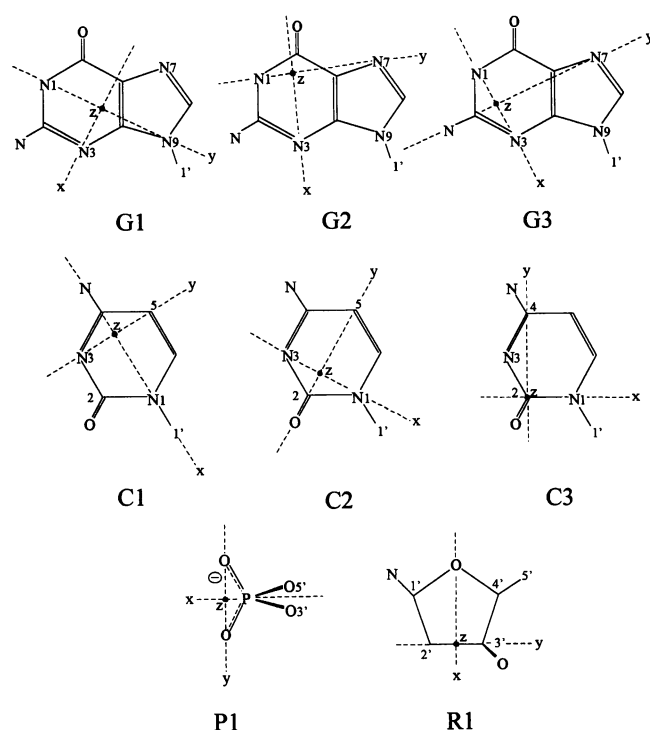


FIGURE 4 Principal axes (x , y , and z) of the local Raman tensors representing selected base, sugar, and phosphate group vibrations of RNA, as described in the text and Tables 4–6. The coordinate systems are designated G1, G2, and G3 for purine ring vibrations; C1, C2, and C3 for pyrimidine ring vibrations; P1 for phosphodiester and phosphodiester stretching vibrations; and R1 for ribose ring vibrations. Within the limits of the present experimental data, these coordinate systems (or alternates involving only permutations of the principal axes) represent all reasonable choices for the Raman tensor calculations.

Table 5 or 6 (column 1), we list the RNA residue to which it is assigned (column 2), the principal axis system (column 3) with respect to which the tensors (columns 4 and 5) have been evaluated, and the theoretically computed I_{bb}/I_{cc} (column 6) and I_{bb}/I_{bc} (column 7) values that correspond to the tensors. The theoretical I_{bb}/I_{cc} and I_{bb}/I_{bc} values were obtained as described previously (Thomas et al., 1995) using direction cosines ($l_x, m_x, \dots, m_z, n_z$) calculated for each principal axis system of Table 4 and atomic coordinates of A RNA (Arnott et al., 1972). They are represented in Fig. 5 as contour maps in r_1 - r_2 space. Comparison of the calculated values of I_{bb}/I_{cc} and I_{bb}/I_{bc} (columns 6 and 7 of Tables 5 and 6) with the experimentally determined values (columns 3 and 4 of Tables 2 and 3) shows that the tensors accurately account for all of the polarized Raman intensity ratios.

Because of the high precision in experimentally determined I_{bb}/I_{cc} and I_{bb}/I_{bc} ratios and the larger experimental uncertainties in depolarization ratio measurements, the former were employed as the primary basis for calculating Raman tensors. Nevertheless, most of the calculated depolarization ratios (column 8 of Tables 5 and 6) agree satisfactorily with the experimental values (column 5 of Tables 2 and 3).

TABLE 5 Shapes and orientations of Raman tensors of dsRNA and calculated polarized Raman intensity ratios

Band (cm^{-1})	Residue	Axes	r_1	r_2	I_{bb}/I_{cc}	I_{bb}/I_{bc}	ρ
541	ribose	R1	1.14	4.05	1.02	4.72	0.12
598	C	C3	-1.65	4.63	2.77	6.05	0.45
629	C	C3	-1.94	3.79	1.26	2.63	0.53
			5.17	-2.32	1.26	2.60	0.52
668	G	G1	0.60	4.74	3.69	11.80	0.18
724	A	G1	0.07	4.23	2.56	10.09	0.22
785	C, U	C2	4.0	0.24	2.46	10.79	0.19
813	P	P1	1.34	2.64	1.23	18.0	0.05
848	ribose	R1	1.09	3.1	1.02	6.95	0.08
918	ribose	R1	2.68	7.15	0.69	5.29	0.13
1101	P	P1	4.24	8.02	1.00	8.05	0.11
1250	C	C1	6.38	-1.68	2.78	4.69	0.42
1337	A	G2	-1.61	4.9	2.69	5.81	0.44
1377	A, G	G2	-1.25	3.79	1.70	5.84	0.41
1482	G, A	G1	0.86	4.72	4.05	13.12	0.16
1573	G	G1	0.0	6.2	4.10	8.00	0.25
	A	G1	-8.5	3.95	4.10	7.98	0.67
1686	U	C1	4.31	0.25	3.20	13.0	0.20
1720	G	G2	4.24	0.49	3.90	18.8	0.17

The Raman tensors presented in Tables 5 and 6 (and illustrated in Fig. 6) are based upon the chosen principal axes of Fig. 4. Additional assumptions are the following: 1) experimental errors in I_{bb}/I_{cc} and I_{bb}/I_{bc} caused by possible misalignment of fibers are negligibly small; 2) the A RNA coordinates of Arnott et al. (1972) are appropriate for the present calculations on dsRNA from bacteriophage $\phi 6$; and 3) small differences in ρ values are attributable to deformations of the tensors upon going from fiber to solution. If these assumptions are valid, then the Raman tensors obtained here should be sufficient for determining the orientations of base, sugar, and phosphate residues in any double-stranded A helix, and should also be of use in determining

TABLE 6 Shapes and orientations of Raman tensors of deuterated dsRNA and calculated polarized Raman intensity ratios

Band (cm^{-1})	Residue	Axes	r_1	r_2	I_{bb}/I_{cc}	I_{bb}/I_{bc}	ρ
540	ribose	R1	0.73	3.35	1.30	4.24	0.12
571	C	C3	-1.39	3.58	1.57	4.94	0.44
664	G	G1	0.78	5.54	4.66	11.2	0.18
716	A	G1	0.03	4.52	2.76	9.48	0.23
777	C, U	C2	4.12	0.20	2.50	10.3	0.20
812	P	P1	1.45	3.45	1.34	11.2	0.08
852	ribose	R1	1.13	2.84	0.99	8.72	0.07
912	ribose	R1	5.05	12.0	0.57	5.58	0.14
1101	P	P1	3.27	6.26	1.04	9.04	0.10
1255	C	C1	4.26	-0.48	2.26	8.66	0.29
1343	A	G2	-0.65	3.7	2.27	11.1	0.31
1372	A, G	G2	-0.7	3.05	1.45	9.0	0.32
1476	G, A	G1	0.7	3.7	2.92	15.6	0.14
1575	G	G2	-0.3	4.2	3.4	15.9	0.26
	A	G1	-5.76	2.06	3.25	15.6	0.64
1689	G	G1	3.35	0.7	3.10	26.7	0.12
1689	U	C1	3.22	1.03	3.15	26.5	0.09

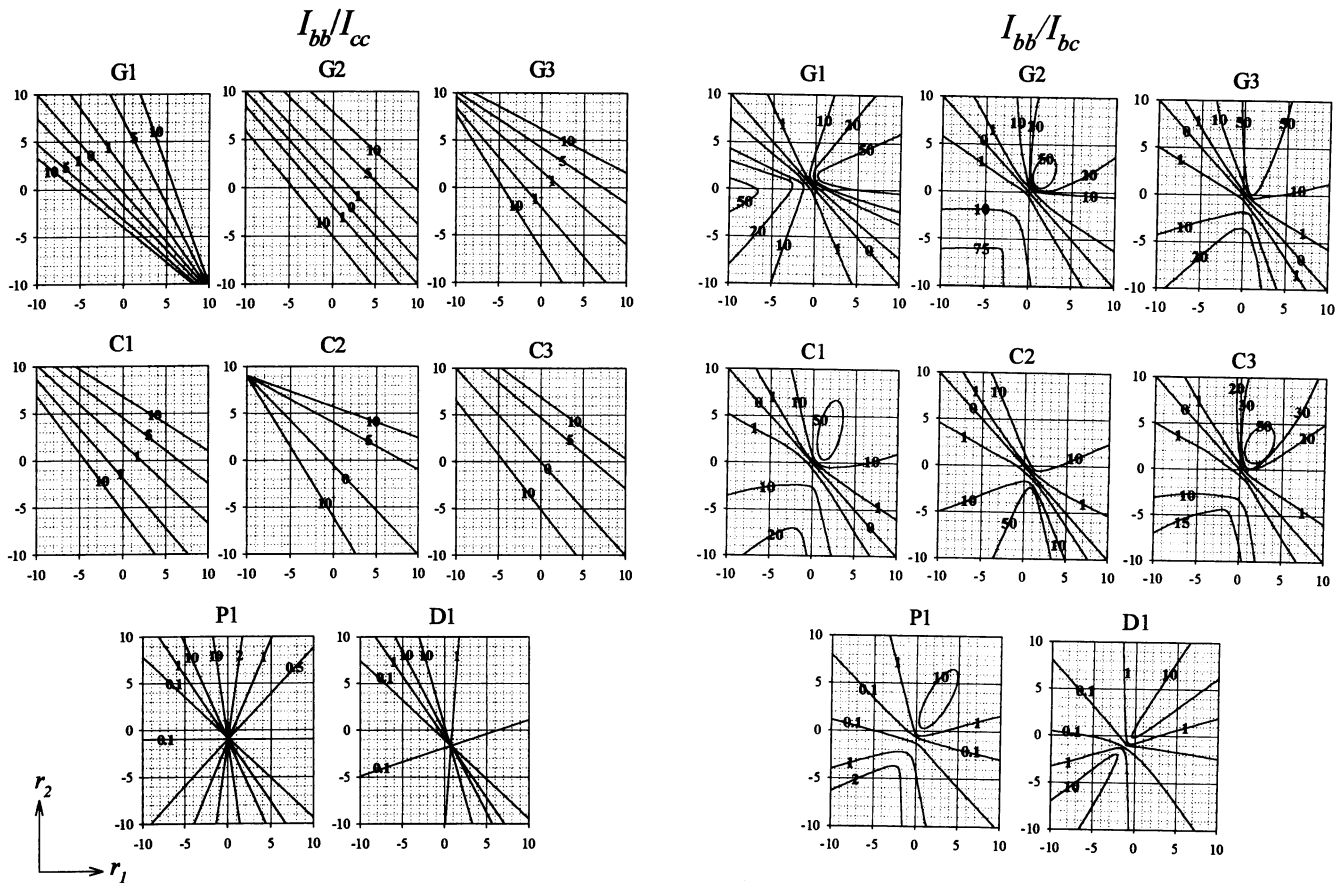


FIGURE 5 Calculated I_{bb}/I_{cc} (left) and I_{bb}/I_{bc} (right) values represented in (r_1, r_2) -space for A RNA. Calculations are based upon the coordinates of Arnott et al. (1972).

the orientations of the helix itself when incorporated into a larger assembly.

In the following sections we comment further upon specific Raman tensors of the RNA Raman bands (in cm^{-1} units) of greatest interest. Each of these Raman tensors is represented diagrammatically in Fig. 6.

541 cm^{-1} band

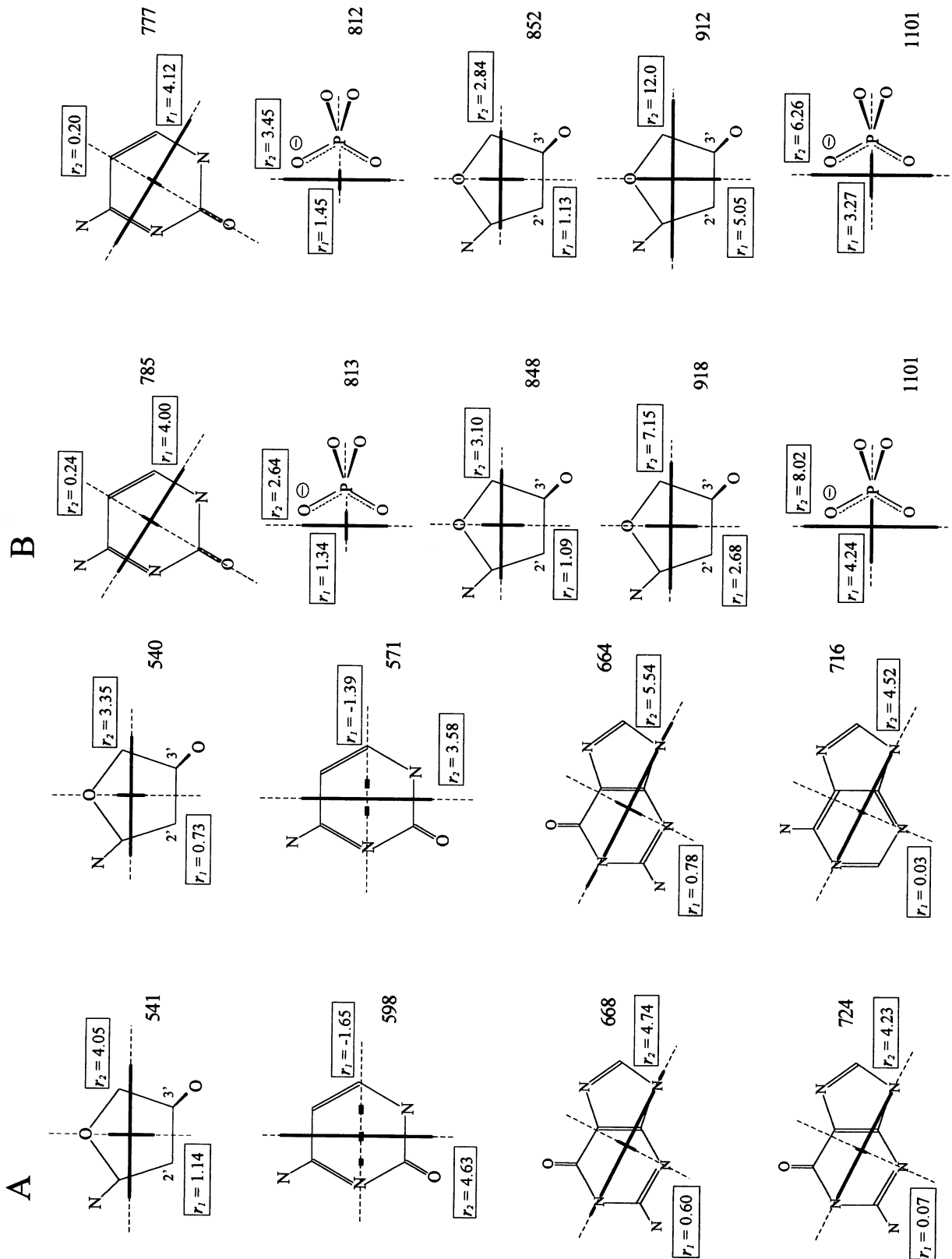
This band is relatively insensitive to deuteration, shifting only to 540 cm^{-1} in dsRNA[D]. No similar band is observed in Raman spectra of A or B DNA (Thomas et al., 1995) or of RNA containing exclusively GC pairs (Lafleur et al., 1972). The fact that $I_{bb} \cong I_{cc}$ suggests that the band arises from a vibration localized in the ribose-phosphate backbone, having its greatest polarizability change along the fiber axis. A reasonable Raman tensor could not be found utilizing axis systems P1, C1, C2, C3, G1, G2, or G3. Only the R1 axis system gives a satisfactory result. On the basis of this result, the band is assigned to a ribose ring vibration, with the greatest change in polarizability occurring along the C2'-C3' bond. The band is most likely sensitive to both stacking and pairing of the bases.

598 cm^{-1} band

The band at 598 cm^{-1} in dsRNA is replaced by a band at 571 cm^{-1} in dsRNA[D]. A similar band is observed in both A and B DNA (Thomas et al., 1995), but not in duplexes containing only AU or AT pairs (Lafleur et al., 1972; Thomas and Benevides, 1985). The similar band at 603 cm^{-1} in crystals of cytidine has been assigned to a ring vibration analogous to the 605 cm^{-1} degenerate vibration of benzene (Ueda et al., 1996). For the cytidine crystal, the largest polarizability change occurs along the C2-C4 line. Consistent results are obtained here for both dsRNA and dsRNA[D].

668 cm^{-1} band

The band at 668 cm^{-1} in dsRNA (664 cm^{-1} in dsRNA[D]) is assigned to a quasi-symmetrical ring-stretching (breathing) mode of the six-membered aromatic ring of guanine (Lord and Thomas, 1967; Thomas, 1970; Lafleur et al., 1972; Tsuboi et al., 1973). The tensor axes could only be fixed using the G1 system. This tensor is anisotropic, with its largest change of polarizability occurring along a line coinciding with the direction of base pairing. However, it is



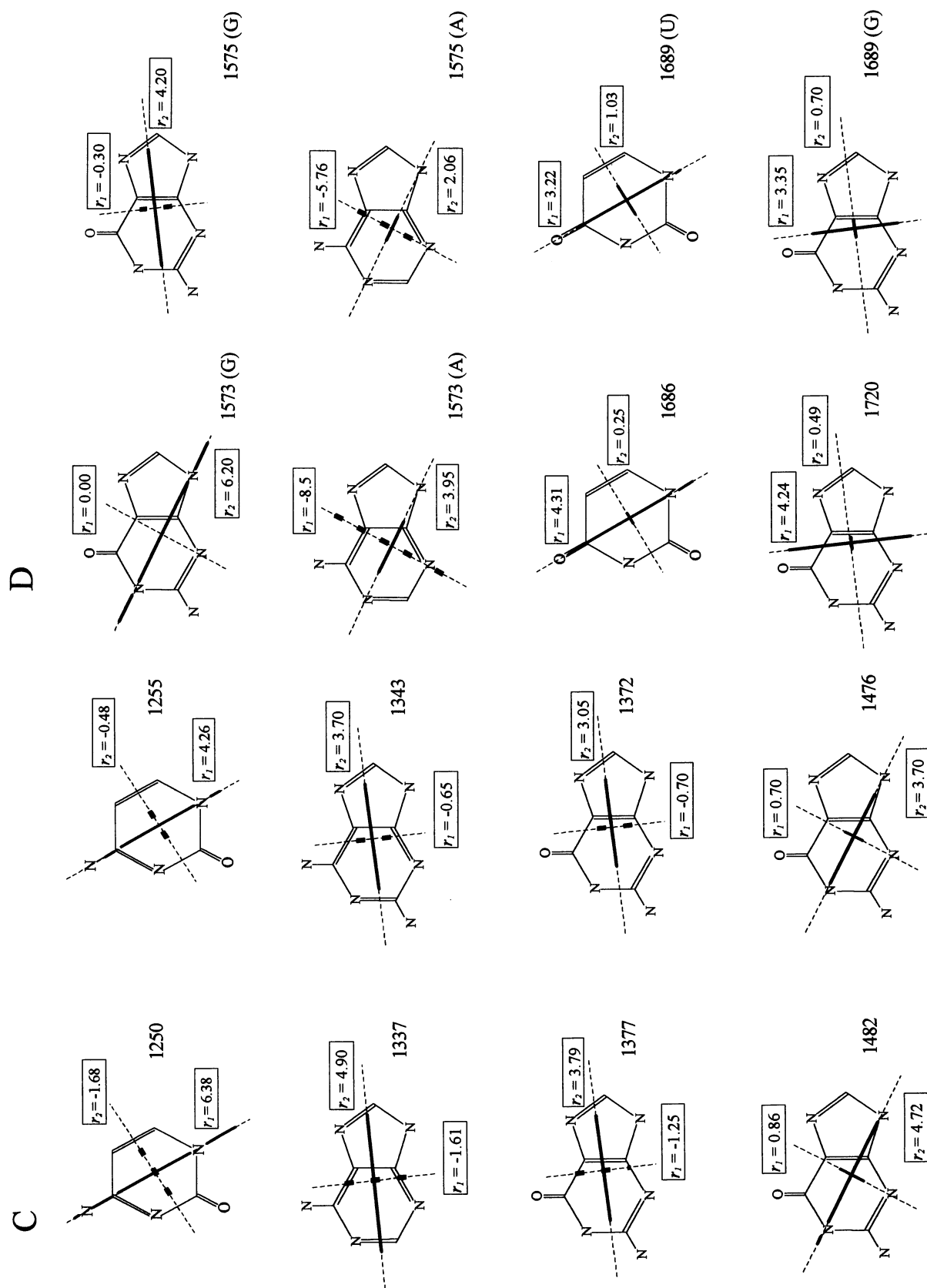


FIGURE 6 Diagrams depicting the local Raman tensors, r_1 and r_2 , determined for 17 vibrational modes of the double-stranded RNA from bacteriophage $\phi 6$. Panels A–D illustrate vibrational modes in the intervals 500–750, 750–1200, 1200–1500, and 1500–1750 cm^{-1} , respectively. In each case, the tensor is depicted for the Raman band of protonated (left column) and deuterated (right column) forms of the RNA duplex. The dashed lines indicate the principal axes of each tensor, in accordance with the definitions for x and y in Fig. 4. Relative magnitudes of r_1 and r_2 are represented by the lengths of the thick lines along the principal axes directions. In cases where r_1 and r_2 are of opposite sign, the negatively signed value is indicated by a broken thick line.

interesting to note that the calculated value of ρ (0.18) (Eq. 1) is significantly larger than the experimental value (0.08), suggesting that the calculated tensor is a first approximation. One explanation for the discrepancy in ρ is that the tensor principal axes, x and y , do not lie precisely in the plane of the base. This would be consistent with other evidence showing that the normal mode in question involves appreciable coupling between the guanine and sugar moieties (Nishimura and Tsuboi, 1986; Thomas et al., 1986).

724 cm^{-1} band

The band at 724 cm^{-1} in dsRNA (716 cm^{-1} in dsRNA[D]) is assigned to the ring breathing mode of adenine (Lord and Thomas, 1967; Thomas, 1970; Lafleur et al., 1972). As in the case of the 668 cm^{-1} band of guanine, the band is quite anisotropic with the largest polarizability oscillation taking place along the direction of base pairing. As in the case of the guanine 668 cm^{-1} band (above), the calculated depolarization ratio (0.22) for the adenine 724 cm^{-1} band suggests a less isotropic tensor than the experimental value (0.09). Again, this may reflect coupling with the sugar moiety.

785 cm^{-1} band

The band at 785 cm^{-1} , which represents overlapping contributions from ring-breathing vibrations of both C and U, shifts to 777 cm^{-1} with deuteration (Lord and Thomas, 1967; Thomas, 1970; Lafleur et al., 1972). Only the C2 axis system satisfactorily fits the tensor to the polarized Raman data. The tensor is highly anisotropic, with the main change in polarizability again taking place along the direction of base pairing. In fibers of both *A* and *B* DNA (Thomas et al., 1995), and in a single crystal of *Z* DNA (Benevides et al., 1993), the corresponding cytosine band (784 cm^{-1}) is also characterized by an anisotropic tensor. On the other hand, an isotropic tensor was found for the corresponding band (793 cm^{-1}) of crystalline cytidine (C1, $r_1 = 3.8$, $r_2 = 3.2$; Ueda et al., 1996). This suggests that the isotropic tensor found only in crystalline cytidine may be a consequence of intermolecular interactions specific to the nucleoside crystal structure.

813 cm^{-1} band

This marker of the *A*-RNA backbone (Thomas, 1970) is not sensitive to deuteration. Although the polarized Raman intensities I_{bb} and I_{cc} are nearly equal ($I_{bb}/I_{cc} = 1.23$), the intensity I_{bc} is non-zero ($I_{bb}/I_{bc} = 18.00$). Therefore, the tensor is moderately anisotropic with the largest oscillation of polarizability occurring along the line connecting oxygen atoms of the PO_2^- group (Fig. 6). This differs from the tensors for backbone markers of *B* DNA (Thomas et al., 1995) and *Z* DNA (Benevides et al., 1993), where the largest oscillations of polarizability occur, respectively,

along the bisector of the $\text{O3}'\text{—P—O5}'$ angle and along the $\text{P—O3}'$ bond.

848 and 918 cm^{-1} bands

Two ring modes of furanose are expected between 850 and 920 cm^{-1} (Tsuboi et al., 1994). In *A* DNA, Raman bands at 882 and 897 cm^{-1} were assigned to the $\text{C3}'\text{-endo}$ deoxyribose ring (Thomas et al., 1995). Only the Raman tensor of the 897 cm^{-1} band was determined and it was found to be much more anisotropic ($r_1 = 2$; $r_2 = 5$) than its counterpart in thymidine ($r_1 = 0.8$, $r_2 = 1.9$; Ushizawa et al., 1996b), an effect attributed to the 3' and 5' phosphoryl substituents (Thomas et al., 1995). In dsRNA, the furanose bands occur at different frequencies, 848 and 918 cm^{-1} , and are far more anisotropic than their *A* DNA counterparts. These effects are attributed tentatively to the additional 2' hydroxyl group of ribose. Deuteration appears to shift the 848 cm^{-1} band to higher frequency (852 cm^{-1}) but has almost no effect on the Raman tensor. For the 918 cm^{-1} band, on the other hand, deuteration produces a shift to lower frequency (912 cm^{-1}) and markedly diminishes the out-of-plane tensor component. It would appear that the latter vibration involves more direct participation of the 2' hydroxyl group.

1101 cm^{-1} band

This vibration is not deuteration sensitive. Based upon the observation that $I_{bb} = I_{cc}$ and $\rho = 0.1$, the tensor is not expected to be highly anisotropic. The high quality of the I_{bb}/I_{bc} data allowed us to evaluate the tensor as given in Fig. 6. The polarizability oscillates along the dioxy $\text{O}\cdots\text{O}$ line with about twice the magnitude of that observed along the bisector of the phosphodiester OPO angle.

1250 cm^{-1} band

The two strong bands of dsRNA in this spectral region (1240 and 1250 cm^{-1}) are replaced by a single band of higher frequency (1255 cm^{-1}) in dsRNA[D]. Both U and C have deuteration-sensitive Raman bands near 1250 cm^{-1} that are dependent upon the furanose conformation. Based upon recent normal coordinate calculations (Tsuboi et al., 1987), the normal modes involve in-plane bending of the C5-H and C6-H protons in an out-of-phase manner (scissoring-type motion). This vibration generates a strong oscillation of the polarizability along the $\text{C5}=\text{C6}$ bond. Replacement of the C5 and C6 protons with deuterium shifts this band to the 800–900 cm^{-1} region (Susi et al., 1973). Thus, the tensor is highly anisotropic.

1337 cm^{-1} band

The band at 1337 cm^{-1} in dsRNA is assigned to adenine residues. Its counterpart in dsRNA[D] is presumably the 1343 cm^{-1} band. Because the values of ρ are relatively large, the tensors should be highly anisotropic. For the

adenine residue in a UpA single crystal (Tsuboi et al., 1995) and for the hypoxanthine residue in an IMP single crystal (Ushizawa et al., 1996a), the corresponding tensors exhibited their greatest polarizability oscillation along the long axis of the purine ring (G2 axis system, Fig. 4). The present tensor calculations for dsRNA show that the G2 axis system is also the most preferable.

The dsRNA fiber also exhibits weak bands at 1297 and 1318 cm^{-1} , which are replaced by a single strong band at 1305 cm^{-1} in dsRNA[D]. Because nucleotides of C, A, and G all contribute significantly to the observed bands, reliable tensor calculations are not feasible.

1377 cm^{-1} band

The very broad band of dsRNA with peak centered at 1377 cm^{-1} is due mainly to overlapping ring vibrations of A and G (Lord and Thomas, 1967). In dsRNA[D], the band complex is shifted to higher frequency with peak position at 1388 cm^{-1} . The Raman tensor calculations parallel those for the 1337 and 1343 cm^{-1} bands of A, discussed above.

1482 cm^{-1} band

The 1482 cm^{-1} band shifts to 1476 cm^{-1} with deuteration and has been assigned to ring vibrations of A and G (Lord and Thomas, 1967). The guanine contribution is the greater, approximately threefold larger than that of A. The band has great diagnostic value, both as a monitor of deuterium-exchange kinetics of the purine C8H group (Benevides et al., 1984) and as an indicator of purine N7 hydrogen bonding interactions (Nishimura et al., 1986; Benevides et al., 1991). It has a distinctively lower depolarization ratio ($\rho = 0.16$) than either the 1337 (0.42) or 1377 cm^{-1} band (0.40). In the single crystal of IMP (Ushizawa et al., 1996a), the greatest oscillation in polarizability is along the N1---N9 line (G1 axis system). Similarly, a highly anisotropic tensor is found for dsRNA and dsRNA[D].

1573 cm^{-1} band

The 1573 cm^{-1} band, which comprises nearly equal contributions from A and G, is little affected by deuteration. In mononucleotides, the depolarization ratio is much higher for adenine ($\rho = 0.64$) (Tsuboi et al., 1995), than for guanine ($\rho = 0.34$) (Ueda et al., 1993). This indicates that even though the A and G modes occur at the same frequency and exhibit similar intensities, their Raman tensors are not equivalent. Two different tensors with similar I_{bb}/I_{cc} and I_{bb}/I_{bc} ratios, but different ρ values have been determined, as shown in Fig. 6.

1686 cm^{-1} band

The 1686 cm^{-1} band of dsRNA is assignable primarily to an in-phase stretching motion of the conjugated C6=C5-C4=O network in uracil, with the largest oscil-

lation in polarizability taking place along the C4=O/C5=C6 direction. The counterpart in dsRNA[D] occurs at 1689 cm^{-1} and overlaps with the C6=O carbonyl stretching mode of G. Not surprisingly, the effective tensors are quite different from one another.

1720 cm^{-1} band

The 1720 cm^{-1} band is highly sensitive to secondary structure, including base pairing interactions. No comparable band occurs in Raman spectra of neutral mononucleotides. In Raman spectra of nucleic acids, the band intensity is weak in B DNA, stronger in A DNA and strongest in dsRNA. A similar Raman band has also been observed in hydrogen-bonded quadruplex structures of guanine-containing DNA and its deuteration shifts have been documented (Miura and Thomas, 1995). If it is assumed that the Raman band at 1720 cm^{-1} in dsRNA is due to the guanine C6=O stretching vibration, and if a tensor with the G2 axis system is assigned, the tensor of Fig. 6 provides a satisfactory fit to the observed I_{bb}/I_{cc} and I_{bb}/I_{bc} intensity ratios. The calculated tensor is consistent with the greatest polarizability change taking place along the C6=O bond. Upon deuteration, the band shifts to lower frequency and becomes overlapped by the more prominent uracil band (above).

SUMMARY AND CONCLUSIONS

In the present study, the shapes and orientations of Raman tensors for all prominent bands of double-helical RNA and its deuterium-exchanged product (dsRNA[D]) have been determined. The dsRNA has been isolated from bacteriophage $\phi 6$. The present approach makes use of accurately measured polarized Raman data (I_{bb} , I_{cc} and I_{bc} spectra) of oriented dsRNA fibers, supplemented with solution depolarization ratios (ρ), to determine three unknown parameters for each prominent Raman band: 1) the orientation of the principal axis system for the tensor; 2) the ratio of tensor principal components, α_{xx}/α_{zz} ($\equiv r_1$); and 3) the ratio of tensor principal components, α_{yy}/α_{zz} ($\equiv r_2$). These local Raman tensors of dsRNA are also compared with tensors determined previously on A, B and Z DNA duplexes. A sufficient library of Raman tensors now exists to provide a basis for reaching general conclusions about tensor characteristics for a number of local vibrations in nucleic acids. The key assumptions in the present application are the applicability of the atomic coordinates of Arnott et al. (1972) to the $\phi 6$ dsRNA structure, the near-perfect orientation of dsRNA in the fibers, and the validity of the adopted principal axis systems.

The Raman tensors corresponding to ring breathing vibrations of A, T, U, G, and C are only moderately anisotropic in character. The three principal tensor components exhibit the same sign, with the main change in polarizability taking place along the direction of Watson-Crick base pairing. In almost every case, the tensor component perpendic-

ular to the base plane (α_{zz}) is intermediate in magnitude between in-plane components (α_{xx} and α_{yy}). The only exceptions occur for Raman tensors of ring breathing vibrations of G and C in the Z-DNA crystal with sequence d(CGCGCG) (Benevides et al., 1993). In this structure, the G and C ring breathing modes exhibit tensors which are somewhat more isotropic in character and which exhibit their smallest component (α_{zz}) perpendicular to the base plane. The basis for this exceptional result on d(CGCGCG) is presently unclear and will be further investigated. One possibility is that the larger distance between successive base pairs in Z DNA affects the α_{zz} tensor component.

For the first time, the shape and magnitude of the Raman tensor for the principal marker (813 cm^{-1} band) of the A-form nucleic acid backbone has been determined. The experimental values of I_{bb}/I_{cc} , I_{bb}/I_{bc} and ρ are duplicated accurately for the 813 cm^{-1} band by use of the P1 principal axis system (Table 4) and r_1 and r_2 values of 1.34 and 2.64, respectively. These results are as expected for a symmetrical stretching vibration which is highly polarized; they are also in accord with assignment of the 813 cm^{-1} mode to an essentially pure O-P-O symmetrical stretching vibration (Thomas, 1970). In contrast to the A-form Raman marker, those for B (834 cm^{-1}) and Z (745, 790 cm^{-1}) forms of the nucleic acid backbone exhibit qualitatively different tensors and the normal modes cannot be considered simply as localized and symmetrical O-P-O stretching vibrations (Thomas et al., 1995; Benevides et al., 1993). We propose that greater vibrational coupling occurs between phosphodiester and furanose moieties in B and Z structures than in the A structure, leading to shifting of the vibration to lower frequency with attendant changes in the shape and orientation of the Raman tensor. This could account for the somewhat unexpected result that the polarizability oscillation for the 813 cm^{-1} vibration in dsRNA is greatest along the O---O line of the PO_2^- group rather than along the bisector of the O3'—P—O5' angle as observed for B DNA (Thomas et al., 1995) or along the P—O3' bond as observed in Z DNA (Benevides et al., 1993).

All orthophosphate diesters exhibit a strong and polarized Raman band in the interval 1080–1105 cm^{-1} , which is diagnostic of the PO_2^- group and due to its symmetrical stretching vibration. In previous work, the Raman tensor for the diagnostic PO_2^- symmetrical stretching vibration of B DNA (1090 cm^{-1}) was shown to be isotropic (Thomas et al., 1995). For the corresponding Raman band of A DNA (1100 cm^{-1}), a unique fit of the data was not possible; however, a nearly isotropic tensor ($r_1 \approx r_2$) was also found to be consistent with the experimental data (Thomas et al., 1995). The present results on the PO_2^- symmetrical stretching mode of dsRNA (1101 cm^{-1}) indicate a more highly anisotropic tensor, with $r_1 = 4.24$ and $r_2 = 8.02$. Thus, the A backbone of dsRNA is more similar to the Z backbone of the d(CGCGCG) crystal, which also exhibits a PO_2^- symmetrical stretching mode (1095 cm^{-1}) with an anisotropic tensor. In the case of the Z DNA crystal the largest polarizability change occurs along a direction perpendicular to

the plane of the PO_2^- group rather than along any in-plane direction (Benevides et al., 1993). On the basis of the accumulated data, we conclude that the tensor characteristics of this band are uniquely dependent upon the helix secondary structure and/or phosphate group local environment. This would account for the distinctive frequency and intensity of the Raman band in different canonical forms of DNA, and would be consistent with the large body of experimental and theoretical evidence on phosphate dialkyl esters (Guan and Thomas, 1996a, b).

Raman tensors of the PO_2^- symmetrical stretching vibration are not alone in being influenced by local environment. Comparison of the present results with those obtained previously on A, B and Z DNA (Benevides et al., 1993; Thomas et al., 1995) indicates subtle differences in Raman tensors for purine and pyrimidine ring vibrations above 1200 cm^{-1} . Although a consistent pattern prevails in distinguishing isotropic from anisotropic tensors, the tensor shapes and magnitudes are influenced by the secondary structure and/or base sequence. We regard this as a "second-order" effect, meaning that the tensors for ring modes above 1200 cm^{-1} , while largely transferable among different structures, exhibit small but significant sensitivity to the base context. The optimal transferability of these tensors is between fibers of A and B DNA (Thomas et al., 1995). Conversely, transferability appears to be most tenuous between A RNA and A DNA. This could reflect the fundamental structural differences between uracil and thymine, as well as the likelihood that the tensors for most bands of the 1200–1600 cm^{-1} interval are dependent upon the nature of the attached sugar. Clearly, further study is needed to understand the observed phenomena.

Finally, the tensor analysis of dsRNA and dsRNA[D] has helped to assign specific vibrational modes of the ribosyl moiety. The furanose ring stretching modes in A RNA are demonstrated to depart greatly from those of A DNA. The corresponding tensors are also greatly different, with those of RNA being far more anisotropic than their DNA counterparts. These effects are attributed to the different C2' substituents in RNA and DNA.

The results obtained in the present study demonstrate that suitably anisotropic Raman tensors exist for all residues of dsRNA, including A, U, G, C, ribose, and phosphate residues. In principle, the orientations of each of these residue types can be determined in dsRNA-containing biological assemblies by use of the method of polarized Raman microspectroscopy and the presently established Raman tensors.

The support of this research by National Institutes of Health Grants GM50776 and GM54378 is gratefully acknowledged.

REFERENCES

- Arnott, S., D. W. Hukins, and S. D. Dover. 1972. Optimized parameters for RNA double-helices. *Biochem. Biophys. Res. Commun.* 48:1392–1399.
- Benevides, J. M., D. Lemeur, and G. J. Thomas, Jr. 1984. Molecular conformations and 8-CH exchange rates of purine ribo- and

- deoxyribonucleotides: investigation by Raman spectroscopy. *Biopolymers*. 23:1011-1024.
- Benevides, J. M., M. Tsuboi, A. H.-J. Wang, and G. J. Thomas, Jr. 1993. Local Raman tensors of double-helical DNA in the crystal: A basis for determining DNA residue orientations. *J. Am. Chem. Soc.* 115: 5351-5359.
- Benevides, J. M., M. A. Weiss, and G. J. Thomas, Jr. 1994a. An altered specificity mutation in the λ repressor induces global reorganization of the protein-DNA interface. *J. Biol. Chem.* 269:10869-10878.
- Benevides, J. M., G. Kukolj, C. Autexier, K. L. Aubrey, M. S. DuBow, and G. J. Thomas, Jr. 1994b. Secondary structure and interaction of phage D108 *Ner* repressor with a 61-base-pair operator: evidence for altered protein and DNA structures in the complex. *Biochemistry*. 33: 10701-10710.
- Brandes, R., A. Rupprecht, and D. R. Kearns. 1989. Interaction of water with oriented DNA in the A- and B-form conformations. *Biophys. J.* 56:683-691.
- Guan, Y., and G. J. Thomas, Jr. 1996a. Vibrational analysis of nucleic acids. IV. Normal modes of the DNA phosphodiester structure modeled by diethyl phosphate. *Biopolymers*. 39:813-835.
- Guan, Y., and G. J. Thomas, Jr. 1996b. Vibrational analysis of nucleic acids. V. Force field and conformation dependent modes of the phosphodiester backbone modeled by diethyl phosphate. *Biophys. J.* 71: 2802-2814.
- Higgs, P. W. 1953. The vibration spectra of helical molecules. Infrared and Raman selection rules, intensities and approximate frequencies. *Proc. R. Soc. Lond. (Biol)*. A220:472-485.
- Lafleur, L., J. Rice, and G. J. Thomas, Jr. 1972. Raman studies of nucleic acids. VII. poly(A)*poly(U) and poly(G)*poly(C). *Biopolymers*. 11: 2423-2437.
- Lamba, O. P., A. H.-J. Wang, and G. J. Thomas, Jr. 1989. Low-frequency dynamics and Raman scattering of crystals of B-, A- and Z-DNA and fibers of C-DNA. *Biopolymers*. 28:677-678.
- Li, T., Z. Chen, J. E. Johnson, and G. J. Thomas, Jr. 1990. Structural studies of bean pod mottle virus, capsid and RNA in crystal and solution states by laser Raman spectroscopy. *Biochemistry*. 29:5018-5026.
- Li, T., D. H. Bamford, J. K. H. Bamford, and G. J. Thomas, Jr. 1993a. Structural studies of the enveloped dsRNA bacteriophage $\phi 6$ of *Pseudomonas syringae* by Raman spectroscopy. I. The virion and its membrane envelope. *J. Mol. Biol.* 230:461-472.
- Li, T., J. E. Johnson, and G. J. Thomas, Jr. 1993b. Raman dynamic probe of hydrogen exchange in bean pod mottle virus: base-specific retardation of exchange in packaged ssRNA. *Biophys. J.* 65:1963-1972.
- Li, Y., G. J. Thomas, Jr., M. Fuller, and J. King. 1981. Investigations of bacteriophage P22 by laser Raman spectroscopy. *Prog. Clin. Biol. Res.* 64:271-283.
- Lord, R. C., and G. J. Thomas, Jr. 1967. Raman spectral studies of nucleic acids and related molecules. I. Ribonucleic acid derivatives. *Spectrochim. Acta*. 23A:2551-2591.
- Mindich, L., and D. H. Bamford. 1988. Lipid containing bacteriophages. In *The Bacteriophages*, Vol. 2. R. Calendar, editor. Plenum Press, New York. 475-516.
- Miura, T., and G. J. Thomas, Jr. 1995. Structure and dynamics of inter-strand guanine association in quadruplex telomeric DNA. *Biochemistry*. 34:9645-9653.
- Nishimura, Y., and M. Tsuboi. 1986. Local conformations and polymorphism of DNA duplexes as revealed by their Raman spectra. In *Spectroscopy of Biological Systems*, Vol. 13. R. J. H. Clark and R. E. Hester, editors. Wiley-Interscience, New York. 177-232.
- Olkkonen, V. M., P. M. Ojala, and D. H. Bamford. 1991. Generation of infectious nucleocapsids in vitro assembly of the shell protein onto the polymerase complex of the dsRNA bacteriophage $\phi 6$. *J. Mol. Biol.* 218:569-581.
- Overman, S. A., M. Tsuboi, and G. J. Thomas, Jr. 1996. Subunit orientation in the filamentous virus Ff (fd, f1, M13). *J. Mol. Biol.* 259:331-336.
- Prescott, B., W. Steinmetz, and G. J. Thomas, Jr. 1984. Characterization of DNA secondary structure by Raman spectroscopy. *Biopolymers*. 23: 235-256.
- Reilly, K. E., and G. J. Thomas, Jr. 1994. Hydrogen exchange dynamics of the P22 virion determined by time-resolved Raman spectroscopy: effects of chromosome packaging on the kinetics of nucleotide exchanges. *J. Mol. Biol.* 241:68-82.
- Steitz, T. A. 1990. Structural studies of protein-nucleic acid interaction: the sources of sequence-specific binding. *Q. Rev. Biophys.* 23:205-280.
- Susi, H., S. Ard, and J. M. Purcell. 1973. Vibrational spectra of nucleic acid constituents. II. Planar vibrations of cytosine. *Spectrochim. Acta*. 29A: 725-733.
- Thomas, G. J., Jr. 1970. Raman spectral studies of nucleic acids. III. Laser-excited spectra of ribosomal RNA. *Biochim. Biophys. Acta*. 213: 417-423.
- Thomas, G. J., Jr., and J. M. Benevides. 1985. An A-helix structure for poly(dA-dT) · poly(dA-dT). *Biopolymers*. 24:1101-1105.
- Thomas, G. J., Jr., J. M. Benevides, S. A. Overman, T. Ueda, K. Ushizawa, M. Saitoh, and M. Tsuboi. 1995. Polarized Raman spectra of oriented fibers of A DNA and B DNA: Anisotropic and isotropic local Raman tensors of base and backbone vibrations. *Biophys. J.* 68:1073-1088.
- Thomas, G. J., Jr. 1986. Applications of Raman spectroscopy in structural studies of viruses, nucleoproteins and their constituents. In *Spectroscopy of Biological Systems*, Vol. 13. R. J. H. Clark and R. E. Hester, editors. John Wiley and Sons, New York. 233-309.
- Thomas, G. J., Jr., and M. Tsuboi. 1993. Raman spectroscopy of nucleic acids and their complexes. *Adv. Biophys. Chem.* 3:1-70.
- Tsuboi, M., T. Ikeda, and T. Ueda. 1991. Raman microscopy of a small uniaxial crystal: tetragonal aspartame. *J. Raman Spectrosc.* 22:619-626.
- Tsuboi, M., Y. Nishimura, A. Y. Hirakawa, and W. L. Peticolas. 1987. Resonance Raman spectroscopy and normal modes of the nucleic acid bases. In *Biological Applications of Raman Spectroscopy: Resonance Raman Spectra of Polyenes and Aromatics*, Vol. 2. T. G. Spiro, editor. Wiley-Interscience, New York. 109-179.
- Tsuboi, M., S. A. Overman, and G. J. Thomas, Jr. 1996. Orientation of tryptophan-26 in coat protein subunits of the filamentous virus Ff by polarized Raman microspectroscopy. *Biochemistry*. 35:10403-10410.
- Tsuboi, M., S. Takahashi, and I. Harada. 1973. Infrared and Raman spectra of nucleic acids: vibrations in the base residues. In *Physico-Chemical Properties of Nucleic Acids*, Vol. 1. J. Duchesne, editor. Academic Press, New York. 92-145.
- Tsuboi, M., T. Ueda, K. Ushizawa, and N. Nagashima. 1995. Raman tensor of adenine residue for the 1580 cm^{-1} vibration and its orientation in a biopolymer. *J. Raman Spectrosc.* 26:745-749.
- Tsuboi, M., T. Ueda, K. Ushizawa, Y. Sasatake, A. Ono, M. Kainosho, and Y. Ishido. 1994. Assignments of the deoxyribose vibrations: isotopic thymidine. *Bull. Chem. Soc. Jpn.* 67:1483-1484.
- Tuma, R., J. H. K. Bamford, D. H. Bamford, M. P. Russell, and G. J. Thomas, Jr. 1996a. Structure, interactions and dynamics of PRD1 virus. I. Coupling of subunit folding and capsid assembly. *J. Mol. Biol.* 257:87-101.
- Tuma, R., J. H. K. Bamford, D. H. Bamford, and G. J. Thomas, Jr. 1996b. Structure, interactions and dynamics of PRD1 virus. II. Organization of the viral membrane and DNA. *J. Mol. Biol.* 257:102-115.
- Tuma, R., P. E. Prevelige, and G. J. Thomas, Jr. 1996c. Structural transitions in the scaffolding and coat proteins of P22 virus during assembly and disassembly. *Biochemistry*. 35:4619-4627.
- Ueda, T., K. Ushizawa, and M. Tsuboi. 1993. Depolarization of Raman scattering from some nucleotides of RNA and DNA. *Biopolymers*. 33:1791-1802.
- Ueda, T., K. Ushizawa, and M. Tsuboi. 1996. Local Raman tensors of cytidine and their orientations in poly(rI) · poly(rC). *J. Mol. Struct.* 379:171-187.
- Urabe, H., H. Hayashi, Y. Tominaga, Y. Nishimura, K. Kubota, and M. Tsuboi. 1985. Collective vibrational modes in molecular assembly of DNA and its application to biological systems. Low frequency Raman spectroscopy. *J. Chem. Phys.* 82:531-535.
- Ushizawa, K., T. Ueda, and M. Tsuboi. 1996a. Polarized micro Raman spectroscopic studies of nucleic acid: local Raman tensors in inosine-5'-monophosphoric acid and the orientation of hypoxanthine residue in poly(rI) · poly(rC) fiber. *Nucleosides Nucleotides*. 15:569-584.
- Ushizawa, K., T. Ueda, and M. Tsuboi. 1996b. Raman scattering tensors of thymidine. *J. Mol. Struct.* (in press).